



OPEN

Characterization and performance evaluation of Cu-based/TiO₂ nano composites

D. Saber¹✉, Kh. Abd El-Aziz², Bassem F. Felemban², Abdulaziz H. Alghtani², Hafiz T. Ali², Emad M. Ahmed³ & M. Megahed⁴

Copper and copper alloys are used in industrial applications and food contact surfaces due to their desirable properties; copper metal matrix composites have been exciting researchers' attention in recent years since they can offer many valuable characteristics. The present study investigated the effects of the TiO₂ nanoparticles addition with different weight percent on the hardness and corrosion behavior of copper nanocomposites. The powder metallurgy method was used to fabricate the Cu/TiO₂ reinforced with different weight fractions of TiO₂ nano particles up to 12 wt.%. The corrosion behavior of fabricated specimens is evaluated using potentiodynamic polarization curves and electrochemical impedance spectroscopy in different solutions. These solutions were 3.5wt.% NaCl, 0.5 NaOH and 0.5 M H₂SO₄ reflected different pH. The results showed that the addition of TiO₂ nano particles improves pure copper's hardness. The hardness of pure copper increased from 53 to 91 HV by adding 12 wt.% TiO₂. The corrosion current density (I_{corr}) of copper nanocomposites test specimens was higher than I_{corr} of pure copper in all test solutions. As TiO₂ nano particles increase, the corrosion resistance of Cu nano composites decreased. All test specimens exhibited little corrosion current density in 3.5 wt.% NaCl solution as compared with other test solutions.

Copper (Cu) and copper alloys are commonly used in industrial applications. Various factors as excellent thermal and electrical conductivities, corrosion resistance, aesthetic appearance, and antimicrobial properties make copper materials are suitable for use in the food sector¹⁻³. Cu is commonly used in heating and cooling systems, pipelines for domestic and industrial water utilities containing seawater⁴. On the other hand pure copper suffers from low hardness, low strength under tensile load, and poor wear resistance. For that reason, one of the potential solutions for these weaknesses is the addition of different particles as reinforcement, and produce copper matrix composite⁵. Presently, metal matrix composites are producing a wide range of interest in the future materials, which are the best alternate over the traditional materials⁶⁻⁹. At the present time, it is well known that better properties for copper metal matrix composites could be produced by proper reinforcement selection. Different ceramic materials like SiC, Al₂O₃, ZrB₂, ZrO₂, TiO₂ and TiB₂ have been used as reinforcement particles in the copper matrix. The addition of these reinforcements to copper has led to the improvement of mechanical properties, which have been stated by researchers¹⁰⁻²³. Elmahdy et al.⁵ reported that, addition 10 wt.% ZrO₂ to Cu-, achieved the microhardness (146.5 HV). Zhang et al.¹⁷ have prepared the ZrB₂ reinforced Cu-matrix composites with more than 120 HV hardness. Wang et al.¹⁸ prepared the ZrB₂ reinforced Cu-matrix composites with more than 100 HV hardness. Sreedharan et al.¹⁹ found that, the hardness of copper increased by increasing B₄C nanoparticles addition. Fathy et al.²⁰ reported that the hardness of copper increased by increasing Al₂O₃ nanoparticles addition. Efe et al.²¹ reported that the hardness of copper increased by increasing SiC nanoparticles addition. Although there are many studies that have focused on investigating the effect of nanoparticles on the properties of copper, there are few of them that have been interested in studying Cu matrix composites reinforced with TiO₂ particles^{10,11}. Copper as a metal matrix composites reinforced with TiO₂ particles are promising materials because of their excellent mechanical and physical properties like good electrical and thermal conductivity and strength at high temperature. Moghanian et al.¹⁰ studied the effect of addition 1–3 wt.% of TiO₂ to copper. They found that, the hardness of Cu/TiO₂ nanocomposite increased by increasing TiO₂ amount. Sorkhe et al.²³ the hardness of Cu/TiO₂ nanocomposite increased by increasing nano particles up to 5 wt.% TiO₂.

¹Industrial Engineering Program, Department of Mechanical Engineering, College of Engineering, Taif University, P.O. Box 11099, Taif 21944, Saudi Arabia. ²Department of Mechanical Engineering, College of Engineering, Taif University, P.O. Box 11099, Taif 21944, Saudi Arabia. ³Department of Physics, College of Science, Taif University, Taif 21944, Saudi Arabia. ⁴Department of Mechanical Design and Production Engineering, Faculty of Engineering, Zagazig University, P.O. Box 44519, Zagazig, Egypt. ✉email: dselsayed@tu.edu.sa

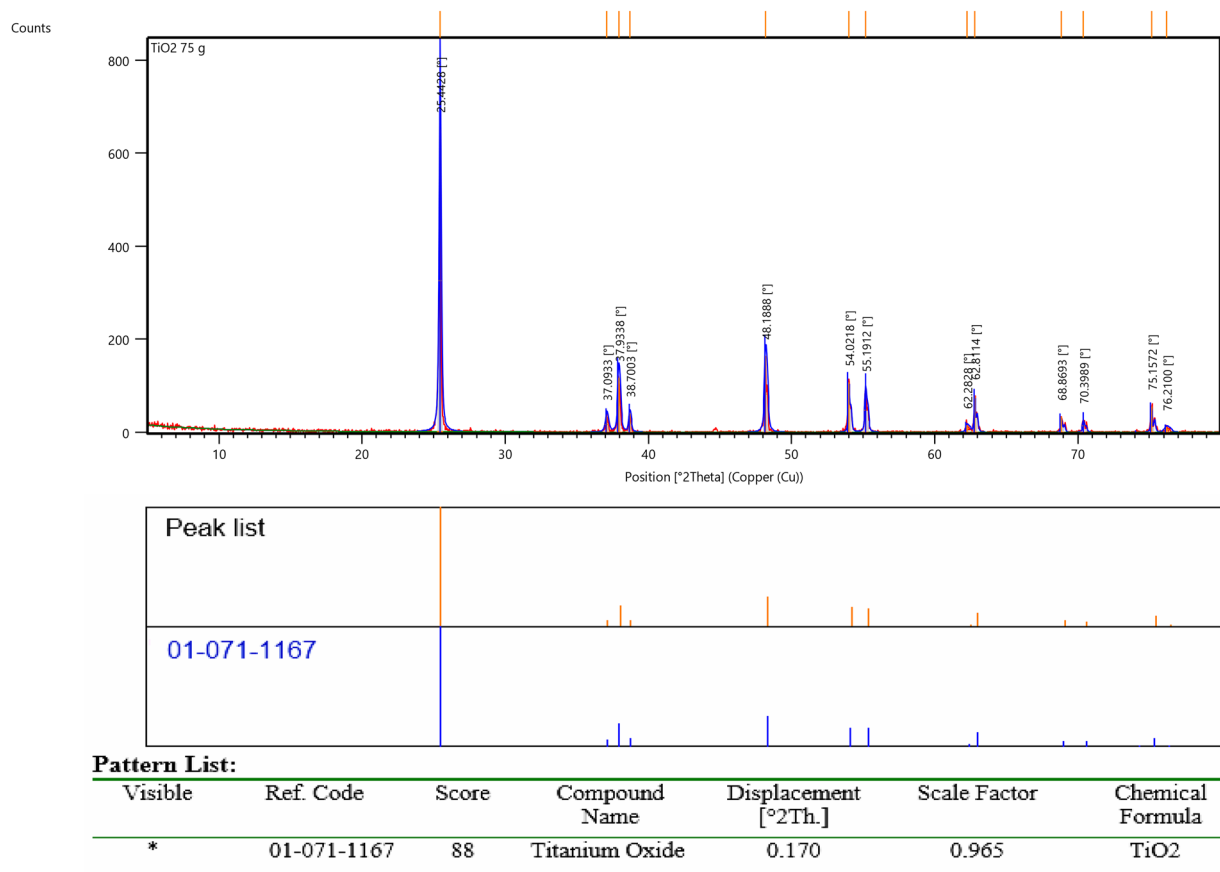


Figure 1. Qualitative XRD analysis of Nano-Titanium Oxide (TiO₂) used as a reinforcement in Cu-based nanocomposites.

The effect of nanoparticles reinforcements on the corrosion behavior of metal matrix composites is still unclear. Addition of nanoparticles reinforcements may increase or decrease the corrosion resistance of composite materials^{23–26}. The corrosion behavior of Cu in aqueous solutions is depending on pH and associating with the morphology of the surface films formed. Few studies have been published about the corrosion behavior of copper composites materials with nanoparticles addition. Saber et al.²⁴ found that, in both 3.5wt.%NaCl and 0.5 M H₂SO₄ solutions, the corrosion rate of Cu/Al₂O₃ nanocomposite increased with increasing Al₂O₃ content Ghazi et al.²⁷ noted that, increasing in SiC as a reinforcement of copper matrix composites, caused severe corrosion at the matrix interface. On the other hand Baghani et al.²⁸ stated that, the corrosion current density for the Cu–Zn–Al₂O₃ nanocomposite is less than that for the Cu–Zn alloy. It was observed from the investigations made by Hosseini et al and Rajesh et al.^{13,29} that the corrosion rate of pure copper and copper coated with TiO₂ were higher compared to Cu/Al₂O₃ composites. Ajeel et al.³⁰ confirmed that the reinforced copper alloy with 3 wt.% of Al₂O₃ and TiO₂ has a lower corrosion rate than reinforced copper alloy reinforced with 1.5 wt.% of Al₂O₃ and TiO₂. While the reinforced alloys with 1.5 wt.% of Al₂O₃ and TiO₂ has lower corrosion rate compared to the copper alloy. Raghav et al.³¹ studied the corrosion of copper–TiO₂ nanocomposite coatings on steel. From this study it is concluded that the steel coating with Cu–25TiO₂ nanocomposite shows better corrosion resistance, than the steel coating with Cu–20TiO₂ nanocomposite.

In the present study, the Cu/TiO₂ reinforced with different weight fractions of TiO₂ nano particles (0, 4, 8, 12) wt.% were fabricated by powder metallurgy method. The corrosion behavior of fabricated Cu nanocomposites is evaluated. The corrosion behavior is studied using potentiodynamic polarization curves and electrochemical impedance spectroscopy (EIS) in 3.5 wt.% NaCl, 0.5 NaOH and 0.5 M H₂SO₄ solutions. In addition, the effect of TiO₂ nanoparticles on the hardness of Cu nanocomposites is determined. The change in density of copper due to TiO₂ nanoparticles addition is also determined.

Experimental work

Metal matrix composites (MMCs) containing TiO₂ nanoparticles with an average particle size of about 80 nm as reinforcements and high purity Cu powder (99% purity and average particle size of 20 μm) as a matrix were prepared by using powder metallurgy method. The chemical analysis of the TiO₂ nano powder was determined using XRD measurements (Bruker D8 advance diffractometer with a Cu-tube operated at 40 kV and 40 mA). Figure 1 presents the result of qualitative XRD peaks' profile and phase analysis of the TiO₂ nano powder used as reinforcement in this study. The metal matrix nanocomposites with weight fractions of 0, 4, 8 and 12 wt.%

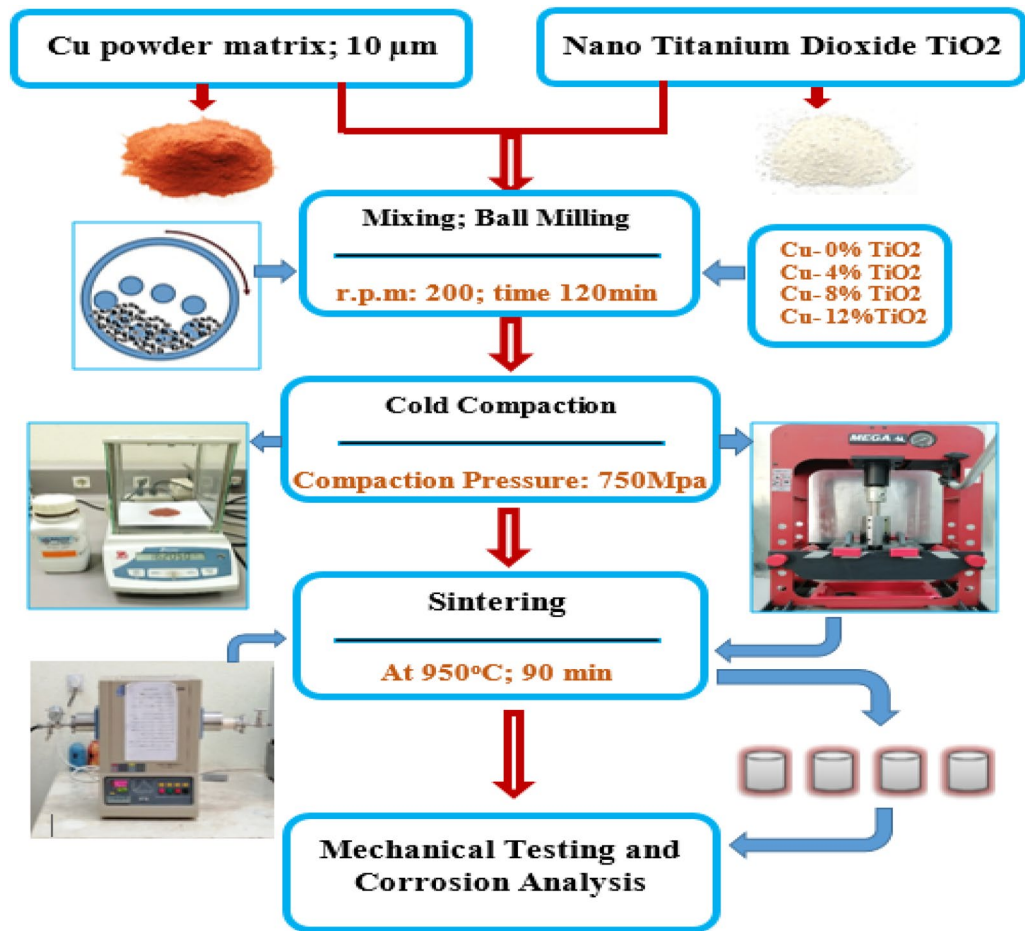


Figure 2. Flow chart and Schematic presentation showing the fabrication path of the present work.

of TiO₂ particles were produced. Different weight percentage of Nano TiO₂ particles was mixed with copper powder using ball mill. Nanocomposite powders were prepared in a way to justify good distribution of the reinforcement particles in the matrix material. For uniform distribution of the reinforcement particles in Cu matrix material, a planetary ball mill (Retsch PM400) for a period of 120 min, with a milling speed of 200 rpm to obtain a uniform distribution of particles was used. The mixed powder of copper and Nano TiO₂ powder is poured into the cylindrical steel mold with an average internal diameter of 18 mm, external diameter of 60 mm and a height of 80 mm. The powders were compressed at compacted pressure of 700 MPa using hydraulic press with the capacity of 25 ton to prepare the cold compacts from the nanocomposite powders. D2 die steel was used as die material. All specimens after compaction were sintered at 950 °C, for 2 h, in a tube furnace chamber, where the flow of Ar gas was provided²⁶. The flowchart of the experimental setup of the Cu/TiO₂ nanocomposites fabrication path is shown in Fig. 2.

After that, etched with a solution contains 75 ml HCl, 25 ml HNO₃, 5 ml HF, and 25 ml H₂O to reveal their microstructure constituents. The microstructure characteristics at the different positions on the specimen surface are investigated by using an optical microscope and scanning electron microscope (SEM). Bulk density measurement of pure Cu and Cu reinforced by TiO₂ nano particles is obtained by the Archimedes method. On the other hand, the theoretical density is determined using the mixture rule according to the weight fraction of the TiO₂ nano particles Eq. (1). Porosities of the nanocomposites are calculated from difference between the experimental and theoretical density of each sample Eq. (2).

$$\rho_T = f_{cu} \cdot \rho_{cu} + f_p \cdot \rho_p \quad (1)$$

$$porosity = \frac{\rho_T - \rho_{Ex}}{\rho_T} \times 100\% \quad (2)$$

where ρ , f are density and volume fraction or weight fraction. Indices cu , p , T and Ex refer to copper, nano particles, theoretical and experimental, respectively¹⁵.

Microhardness is measured after grinding and polishing processes of the tested specimens using a VHS-1000 microhardness testing machine at load of 100 g. The corrosion of Cu / TiO₂ metal matrix composites was accompanied in 3.5 wt.% NaCl, 0.5 M NaOH and 0.5 M H₂SO₄ aqueous solutions. Distilled water was used to

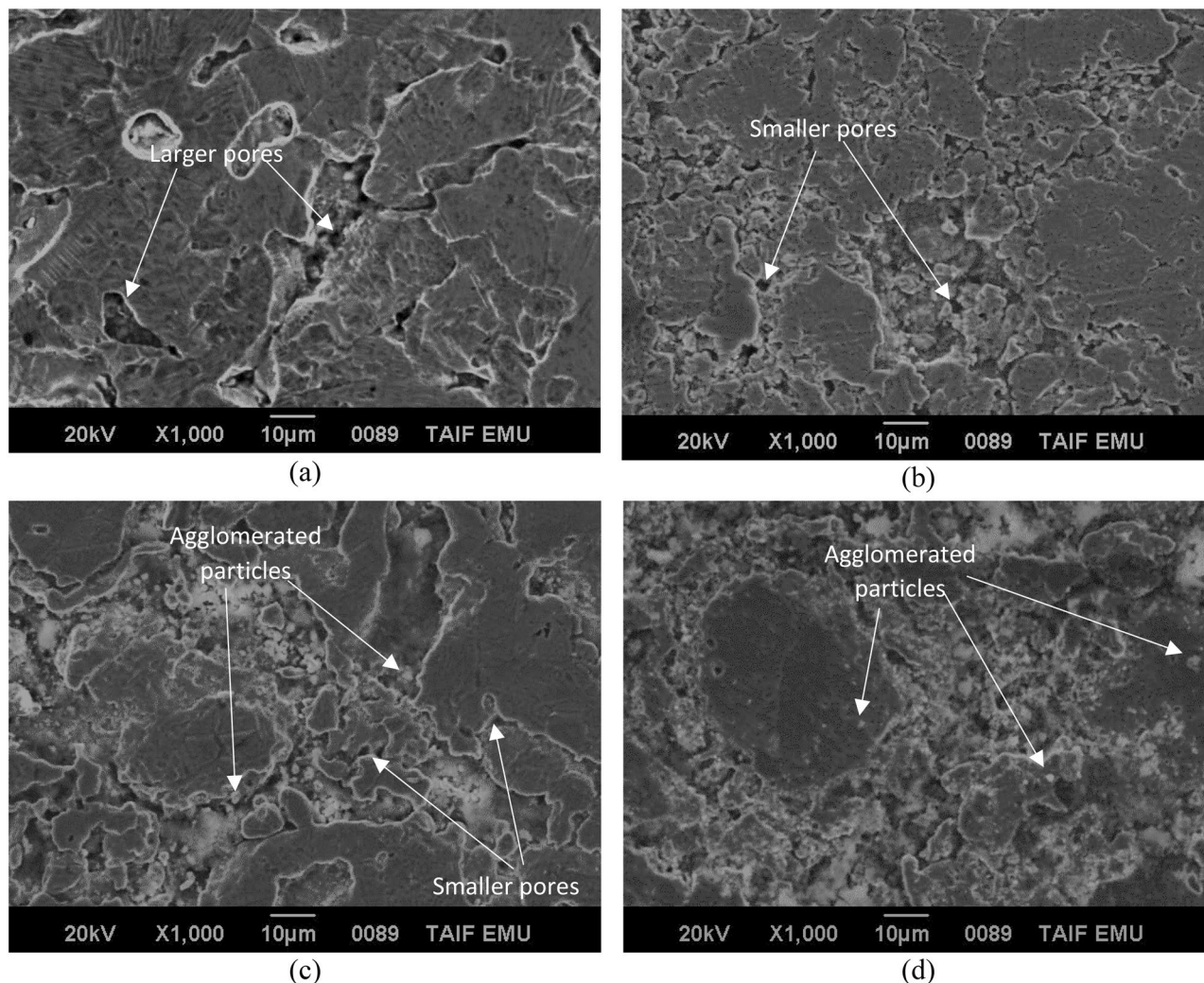


Figure 3. SEM images of the microstructure of Cu/TiO₂ Nano composites; (a) 0% TiO₂, (b) 4% TiO₂, (c) 8% TiO₂, (d) 12% TiO₂.

prepare these solutions prior to each test using. The electrochemical impedance spectroscopy and polarization studies were carried out using Autolab Potentiostat/Galvanostat (PGSTAT 30). The electrochemical impedance spectroscopy measurements were carried out using AC signals of 10 mV amplitude for the frequency spectrum from 100 kHz to 0.01 Hz. A three-electrode cell was used for polarization study. Tafel polarization tests were carried out using a scan rate of 1 mV/min at R.T. The specimens with exposed surface area of 1.7 cm² were used as a working electrode.

Results and discussion

Microstructure characteristics. Figure 3 shows SEM images of the microstructures of synthesized samples of Cu/TiO₂ nanocomposites with 0%, 4%, 8% and 12 wt.% of TiO₂. It can be observed the presence of pores in both pure Cu and nanocomposites. As shown in Fig. 3a the amount and size of forming pores in sample without nano TiO₂ particles, are larger than that in other samples with nano TiO₂ particles. Also, relatively smaller size of forming pores was observed in the SEM image shown in Fig. 3b, as compared with pure Cu. As shown in Fig. 3c and d smaller amounts and size of pores was observed in the intermediate regions between the Cu matrix structure. This may due to the presence of higher amounts of dispersed nano TiO₂ particles in these regions and the Cu matrix, but some of these particles agglomerated with increasing in wt.% of TiO₂ as shown in Fig. 3c,d. This may be attributed that filling capacity of the larger percent of Nano TiO₂ particles inside Cu matrix¹⁹. Figure 4 shows SEM microstructure and EDS spectrum analysis of nanocomposite with 8 wt.% of nano TiO₂ particles. In this figure, SEM micrograph shows the two different regions in the microstructure of the nanocomposite with 8 wt.% of TiO₂, the first displayed the Cu matrix and the second shows nano TiO₂ dispersed particles in Cu matrix. EDS spectrum analysis of nanocomposite with 8 wt.% of nano TiO₂ particles and corresponding elements composition are given in Fig. 4. This confirms the existence of nano TiO₂ particles in Cu matrix structure. Typical higher magnification SEM micrographs and corresponding EDS analysis of Cu/12% TiO₂ nanocomposite with line analysis and EDS mapping are displayed in Fig. 5a–i. As shown in this figure, the results of surface scanning obtained by line analysis and elemental EDS mapping of Cu, Ti, and O elements

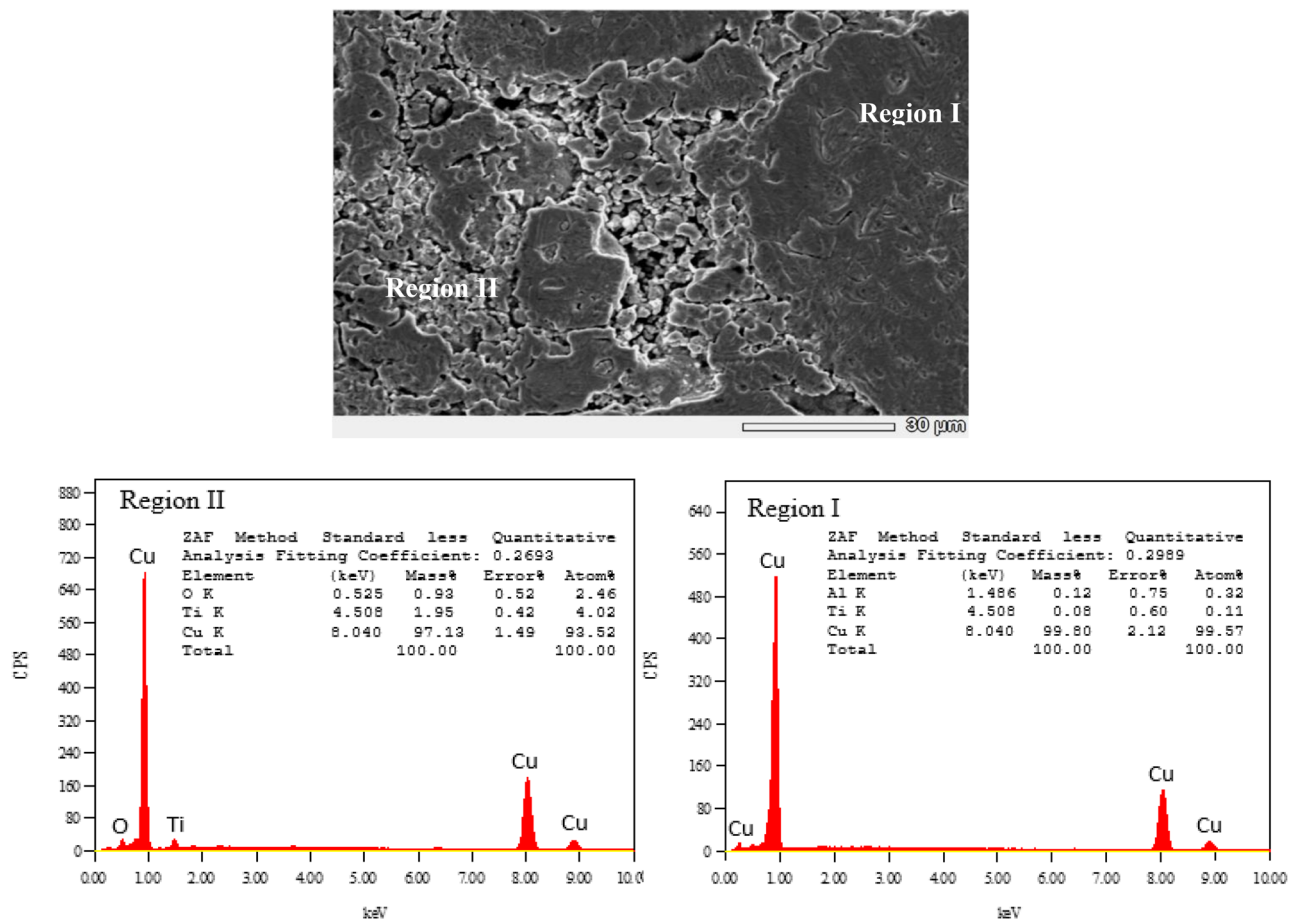


Figure 4. Typical SEM micrograph of different regions and corresponding EDS analysis of Cu/8% TiO₂ nanocomposite.

present in nanocomposites show a uniform distribution of TiO₂ particles in the structure of nanocomposite. But, some of these particles were agglomerated with increasing in wt.% of TiO₂. In this figure it is obvious that copper covers almost the entire surface of the microstructure. The results of surface scanning for Ti and oxygen show that these two elements are present less in the microstructure of the nanocomposite material and the surfaces they inhabit are inter-lapping, which corresponds to the existence of TiO₂ dispersion in the microstructure. In addition, these figure reveals the presence of larger amount of second dispersed phase particles, and the homogeneous dispersion of TiO₂ in the Cu matrix for the nanocomposite specimens.

Density and porosity measurements. Figure 6 presented the correlation between the density and porosity with the different wt.% of TiO₂ Nano-particles. From the figure, it is clear that the theoretical densities of nanocomposites decreased linearly, as expected for the mixtures rule. In addition, the TiO₂ density was lower than the pure Cu. Therefore, any increasing in TiO₂ content must decrease the density of the nanocomposite. The experimental densities are lower than the theoretical densities of all test specimens. This is because the fabricated nanocomposites may contain some porosity. According to Fig. 6 the porosity in nanocomposites decreased gradually with increasing in weight fraction of the TiO₂ Nano-particles. As shown in Table 1 there is no great difference in the porosity between copper and copper nanocomposites. The porosity in copper was 9.6%. while it recorded 9.5% in nanocomposite with 4 wt.% TiO₂. On the other hand a little decrease was noted in nanocomposite with 12 wt.% TiO₂ and recorded about 8.7%. This result was in agreement with Norouzfard et al.¹⁵ and Saif et al.³². Norouzfard et al.¹⁵ fabricated Cu metal matrix composites contain 2.5, 5.5, and 8 wt.% steel nanoparticles. They found that porosity reduces by increasing the steel particles weight fraction. Saif et al.³² using the powder metallurgy technique to fabricate Al/TiO₂ nanocomposite with different content of nano-TiO₂ particles. They found that, by increasing wt% of TiO₂ nanoparticles in the composite matrix the porosity decreases gradually. This can be attributed to diffusion enhancement with increase of sintering time, which causes disappearance of voids between powder particles³³. Moreover, the nanoparticles possess high penetration ability within the pores and voids of the nanocomposite matrix³². Malek et al.³⁴ observed that the number of pores decreased at high sintering temperatures. At the high sintering temperature, the matrix was moved to fill the voids during the consolidation. Kamrani et al.³⁵ suggested that the diffusion of the matrix into the interparticle pores is responsible for this observation.

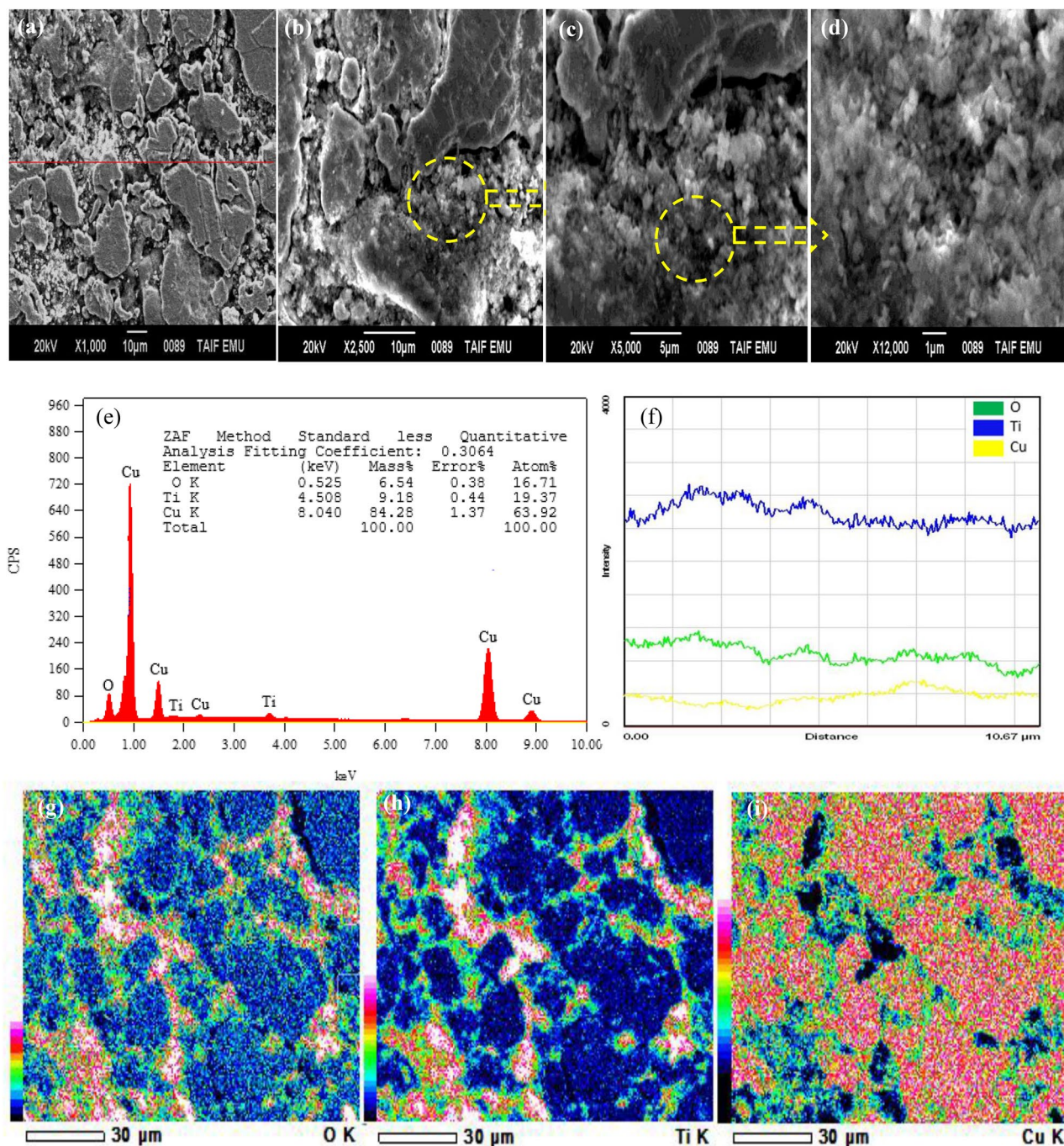


Figure 5. (a) SEM image of nanocomposite containing 12 wt.% TiO₂; (b),(c),(d) Detailed regions of (a) with higher magnifications; EDS spectrum analysis of (a); (f) EDS Line analysis in (a); and (g),(h),(i) EDS mappings of Cu, Ti, and O elements present in (a).

Hardness. Microhardness results of the test specimens are shown in Table 1. As recorded in the table, the microhardness increases with increasing TiO₂ Nano particles. The hardness of pure Cu was 53 HV, and increased to 91 HV in Cu nanocomposite with 12 wt% TiO₂. The addition of 4 wt.% TiO₂ Nano particles improves pure Cu's hardness by 28.3%. Furthermore, by adding of 12wt.% TiO₂ Nano particles improve the hardness of pure Cu by 71.7%. This improvement in the hardness of Cu/TiO₂ nanocomposites is due to the hardness of pure TiO₂ Nano particles was higher than pure Cu. Zawrah et al.¹⁴ concluded that the addition of Al₂O₃ nano particles and their uniform distribution as a strength-enhancing agent. Ning et al.¹¹ prepare Cu/TiO₂ nanocomposite coatings with different content of TiO₂ nano particles. The nanocomposite coating Cu/25 wt.% TiO₂ presented considerably improved microhardness of 218.7 Hv. They suggests that small grain size of nanoparticles has a very strong effect on hardening of Cu/%TiO₂ nanocomposite. The Orowan mechanism plays a remarkable role on

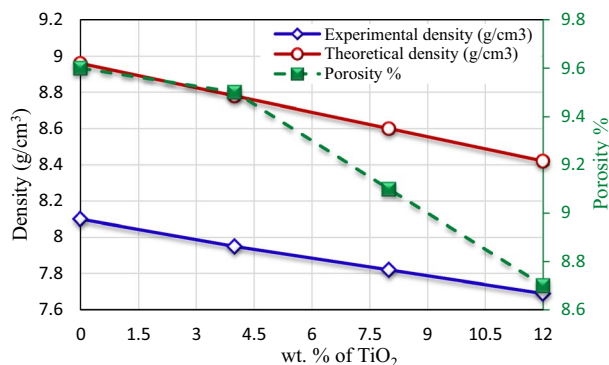


Figure 6. Correlation between both the density and porosity with nano-TiO₂ content.

Nano TiO ₂ -content (wt.%)	Density (g/cm ³) experimental	Density (g/cm ³) theoretical	Porosity%	Microhardness (Hv)
0	8.1	8.96	9.6	53
4	7.95	8.78	9.5	68
8	7.82	8.6	9.1	79
12	7.69	8.42	8.7	91

Table 1. Physical and mechanical properties of Cu/TiO₂ nanocomposites samples.

Nano TiO ₂ content (wt.%)	Electrochemical parameters		Impedance measurements	
	Corrosion current density. (mA/cm ²)	Corrosion potential E _{corr} (-mV)	Ru (ohm)	Rp (ohm)
0	0.01	217	35.33	13.99
4	0.026	215	33.57	9.48
8	0.048	165	16.7	6.53
12	0.063	218	13.8	5.2

Table 2. Corrosion properties of Cu/TiO₂ with different TiO₂ content in 3.5% NaCl solution.

the strengthening of the composites, particularly when the reinforcement size is less than 100 nm²³. The Orowan mechanism proposes that the existence of non-shearable TiO₂ particles within the matrix causes dislocation loop to be left behind after a dislocation line has passed through ceramic TiO₂ particles. It also hinders and/or slows down dislocation motion in copper metal matrix. The internal strain created during the milling process and TiO₂ nanoparticles distributed in a copper matrix act as dislocation movements barrier are the other reasons for hardness increase. Vishwanath et al.³⁷ also explained the reasons for increasing copper's microhardness related to ceramic nanoparticles' addition. They suggested that, by adding of strong and stiff ceramic nanoparticles in the soft ductile copper led to enhancement in the microhardness of copper metal matrix nanocomposites. Another reason is the difference in coefficient of expansion between copper matrix and ceramic nanoparticles can lead to formation of dislocations. The increase in ceramic nanoparticle content led to nanocomposites' dislocation density and acted as obstacles for plastic deformation.

Electrochemical measurements. The polarization curves of the pure Cu and nanocomposite samples with 4, 8 and 12 wt.% TiO₂ after corrosion tests in 3.5% NaCl, 0.5 M NaOH and 0.5 M H₂SO₄ solutions are indicated in Figs. 7, 8 and 9. These figures showed that the addition of TiO₂ in pure Cu matrix increased the anodic and cathodic current densities, and resulted in significant increase in the corrosion current density in all test solutions. Corrosion potential (E_{corr}) and corrosion current density (I_{corr}) were determined by Tafel extrapolation method and they displayed in Tables 2, 3 and 4. The polarization curves Fig. 7 for pure Cu and its nanocomposite specimens in 3.5% NaCl solution shows that active dissolution in anodic region. Also it can be observed that, there is no great difference in E_{corr} between Cu nanocomposite specimens and the pure Cu. As shown in Table 2, I_{corr} of pure Cu in 3.5% NaCl solution was 0.01 mA/cm² and it raised to 0.026 mA/cm² with 4 wt.% TiO₂ nano particles. The severity of corrosive attack continuous increased with the addition of TiO₂ nano particles, and recorded I_{corr} 0.063 mA/cm² for nanocomposite with 12 wt.% TiO₂. The anodic reactions in NaCl solution may be as following reactions³⁶⁻³⁹, at first, the oxidation of copper transforms the copper to Cu⁺ ion (Eq. 3). In the presence of aggressive chloride ions, the reaction between Cl⁻ and Cu⁺ occurs, producing a soluble film on the surface (Eq. 4).

Nano TiO ₂ content (wt.%)	Electrochemical parameters		Impedance measurements	
	Corrosion current density. (mA/cm ²)	Corrosion potential E _{corr.} (- mV)	Ru (ohm)	Rp(ohm)
0	0.67	364	10.67	7.01
4	1.26	455	10.58	5.7
8	1.43	253	7.7	3.64
12	1.93	479	5.2	2.9

Table 3. Corrosion properties of Cu/TiO₂ with different TiO₂ content in 0.5 M NaOH solution.

Nano TiO ₂ content (wt.%)	Electrochemical parameters		Impedance measurements	
	Corrosion current density (mA/cm ²)	Corrosion potential E _{corr.} (- mV)	Ru (ohm)	Rp (ohm)
0	1.2	35.1	5.2	4.9
4	2.7	53.3	4.5	4.6
8	3.6	14.5	2.1	2.9
12	5.3	34.5	1.03	1.87

Table 4. Corrosion properties of Cu/ TiO₂ with different TiO₂ content in 0.5 M H₂SO₄ solution.

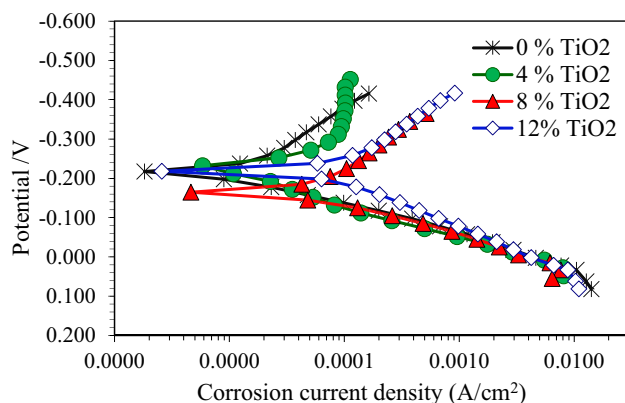


Figure 7. Polarization curves for copper metal matrix composites in 3.5wt.% NaCl solution.



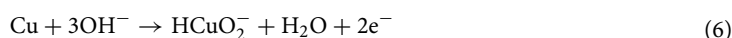
CuCl is an unstable film and instantly reacts with Cl ions and changes to CuCl⁻² as shown in Eq. (5):



The anodic dissolution of copper was organized by both electro dissolution of copper and diffusion of soluble CuCl⁻² to NaCl solution³⁹. As CuCl⁻² formed by anodic dissolution low protection surface is expected³⁸.

Figure 8 shows the polarization curves of pure Cu and its nanocomposite specimens in 0.5 M NaOH solution. This figure indicated a short passive area in the anodic region, specifically for pure Cu and nanocomposite with 4% TiO₂. In addition, the corrosion potential shifts towards more active potentials as TiO₂ nano particles was 12%. From Table 3, E_{corr.} of pure Cu in 0.5 M NaOH solution was - 364 mV, where it was - 479 mV for nanocomposite with 12 wt.% TiO₂. I_{corr.} of pure Cu in 0.5 M NaOH solution was 0.67 mA/cm² and it raised to the highest value of 1.93 mA/cm² with 12 wt.% TiO₂ nano particles.

The anodic behavior of copper in NaOH solution may form an oxide film consisting of either Cu₂O or a duplex layer of Cu₂O and CuO depending on the electrolyte composition and electrochemical conditions⁴⁰. In NaOH solution below 1 M NaOH concentration the direct dissolution of copper as cuprite ions according to either (or both) of the following reactions (Eqs. 6,7):



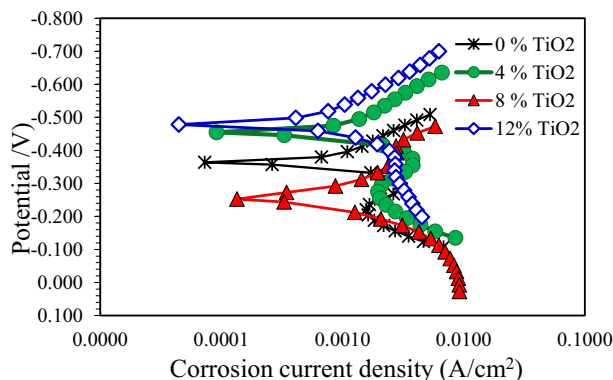


Figure 8. Polarization curves for copper metal matrix composites in 0.5 M NaOH solution.

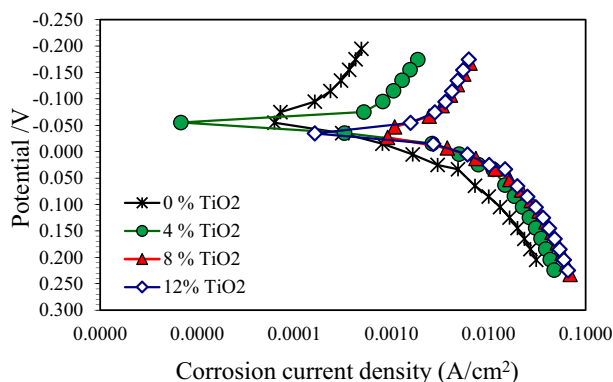
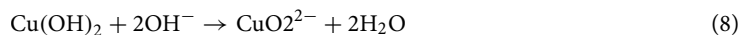


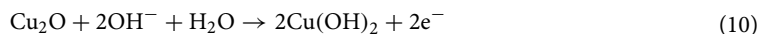
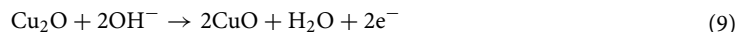
Figure 9. Polarization curves for copper metal matrix composites in 0.5 M H₂SO₄ solution.



and/ or from Cu(OH)₂ through chemical reaction (Eq. 8):



In noble potential the oxidation of cuprous oxide to either (or both) CuO and Cu (OH)₂ according to the following equations:

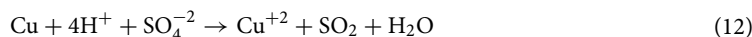


The resulting Cu (OH)₂ may be found in the following equilibrium.



At pH (> 13), thermodynamic equilibrium consideration shows that CuO is unstable and likely dissolves as HCuO₂⁻/CuO₂²⁻⁴¹.

In Fig. 9, it is obvious that the nanocomposite specimens with 4 wt.%, 8 wt.% and 12 wt.% TiO₂ tested in 0.5 M H₂SO₄ solution revealed approximately the same behavior in both anodic and cathodic regions as well as pure Cu. The corrosion reaction of Cu in H₂SO₄ is as follows:



The presence of SO₄²⁻ ions on the surface increases the attack on the copper surface⁴². By comparing the results of corrosion current densities of the investigated nanocomposites and pure Cu in different test solutions, it can be seen that I_{corr} of all specimens is elevated in 0.5 M H₂SO₄ solution in comparison with 3.5 wt.% NaCl and 0.5 M NaOH solutions according to Fig. 10.

The electrochemical impedance spectroscopy is a powerful means that can be used to disentangle the mechanism of electrochemical reactions^{43,44}. Figure 11 shows the Nyquist diagrams for pure Cu and nanocomposites exposed to 3.5 wt% NaCl solution. An arc was observed for pure Cu and nanocomposite with 4 wt.% TiO₂,

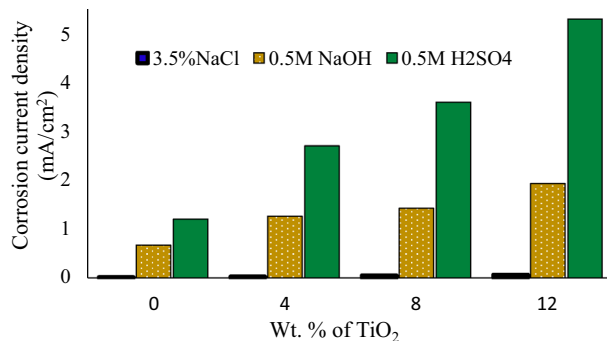


Figure 10. Corrosion current density (i_{corr}) for the three Cu/TiO₂ nanocomposites in different corrosive media (3.5% NaCl, 0.5 M NaOH, and 0.5 M H₂SO₄).

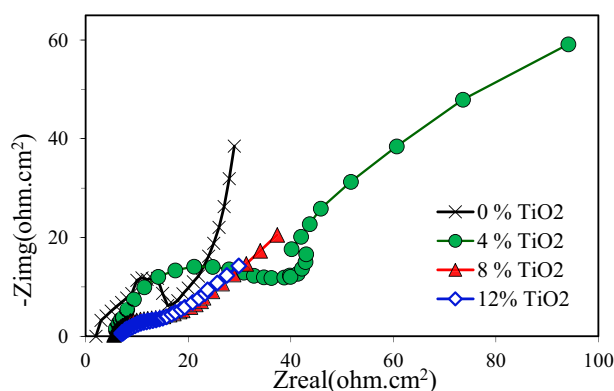


Figure 11. Nyquist plots of copper metal matrix composites in 3.5wt.% NaCl Solution.

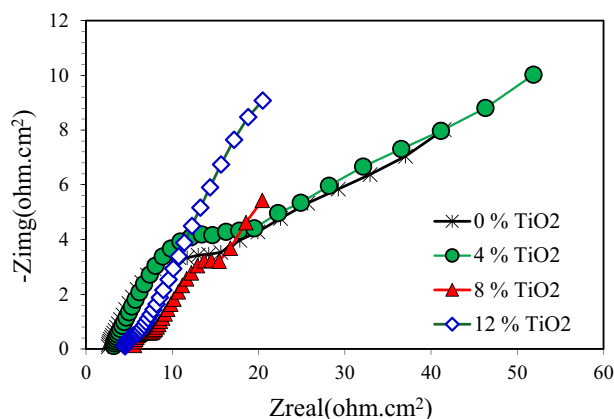


Figure 12. Nyquist plots of copper metal matrix composites in 0.5 M NaOH Solution.

followed by a second arc or tail. From the same figure, it was visible that the nanocomposite Nyquist curve begins approximately at 7 Ohm-cm². This indicates that the migration of the corrosion products by ions to the solution was possible. As a result, this concluded that the nanocomposite a weak and leaky layer that can be dissolved over time permitting the continuous corrosion of the nanocomposite. Figure 12 shows the Nyquist diagrams for pure Cu and Cu nanocomposites exposed to 0.5 M NaOH solution. This figure shows that the Nyquist diagram for pure Cu displays a small semicircle followed by a straight line. Nyquist diagram for Cu nanocomposite with 4% TiO₂ shows a smaller semicircle than pure Cu followed by a straight line. It is obvious from Fig. 13 that, the obtained Nyquist diagram of pure Cu in H₂SO₄ solution produce a semi-circular shape. This indicates that charge transfer essentially controls the corrosion process. The measured electrochemical impedance spectroscopy results for the Cu and Cu nanocomposites in 3.5% NaCl, 0.5 M NaOH and 0.5 H₂SO₄ solutions are summarized in Tables 2, 3 and 4. According to results recorded in Tables 2, 3 and 4, addition of TiO₂ Nano particles to Cu matrix decreased

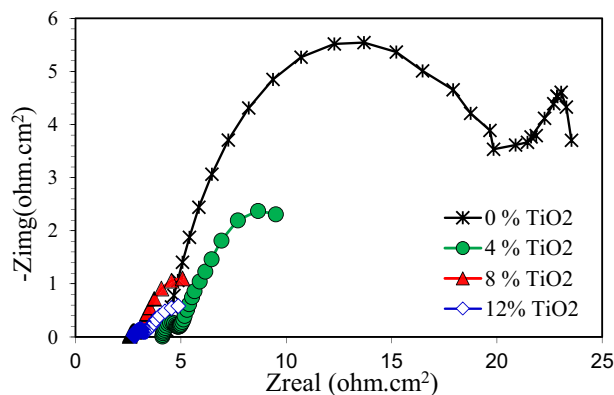


Figure 13. Nyquist plots of copper metal matrix composites in 0.5 M H₂SO₄ Solution.

the resistances R_p and R_u . Another observation, the resistance values R_p and R_u of the specimens in the 3.5% NaCl solution are larger than those in the 0.5 M NaOH and 0.5 H₂SO₄ solutions. Furthermore, the specimens' resistance values R_p and R_u in 0.5 H₂SO₄ solution are the smallest of the three solutions as shown in Tables 2, 3 and 4. The obtained results from polarization curves agree with electrochemical impedance spectroscopy results.

The microstructure of corroded surface of pure Cu and Cu nanocomposite after corrosion test in 3.5% NaCl solution is shown in Fig. 14(a–d). From the figure, it is clear that pure Cu and Cu nanocomposite were attacked by pitting corrosion. In Fig. 14a, pure Cu shows fine pits distributed over the structure, while this pits increased after 4wt.% TiO₂ Nano-particles addition as shown in Fig. 14b. Additionally, these pits increased with increasing TiO₂ Nano-particles addition as shown in Fig. 14a–d. Another observation, Cu-based nanocomposites show that the attacked areas were mainly concentrated around TiO₂ Nano-particles. Moreover, the test solution had slight etching effect on these specimens.

The present results of polarization curves and electrochemical impedance spectroscopy measurements of corrosion behavior of pure Cu and its nanocomposites showed that, the addition of TiO₂ nano-particles to Cu increase corrosion current density in different test solutions. One possible reason for this is that Cu nanocomposites specimens may have a higher initial susceptibility to corrode compared to pure Cu due to the attendance of TiO₂ nano-particles. Harovel⁴⁴ reported that the composite materials may corrode in the interfacial area due to the residual stresses between the particles and the matrix material. Arsenault⁴⁵ reported that, microstructural features may effect the composite materials because of the presence of the reinforcements, and intermetallic phases may be formed around reinforcements. In addition, dissimilarities in the coefficient of thermal expansion between ceramic reinforcement and metal matrix can lead to the generation of dislocations during heating and cooling of metal matrix composite. These dislocations may lead to higher corrosion in metal matrix composite.

The metal matrix and reinforcement exhibit different electrochemical corrosion potentials and characteristics in a neutral salt spray environment^{46,47}. The addition of reinforcement to matrix alloy changes the homogeneity of structure making the matrix more susceptible to localized corrosion⁴⁸. In addition the difference of the reinforcement phase, led to different corrosion behavior of composite materials^{24,27}. Ghazi et al.²⁸ noted that increasing SiC as a reinforcement of copper matrix composites caused severe corrosion at the matrix interface. Saber et al.²⁵ found that, in both 3.5 wt.% NaCl and 0.5 M H₂SO₄ solutions, the corrosion rate of Cu/Al₂O₃ nanocomposite increased with increasing Al₂O₃ content. Rajesh et al. and Hosseini et al.^{13,29} found that the corrosion rate of pure copper and copper coated with TiO₂ was higher than Cu/Al₂O₃ composites. Naseri et al.²³ recommended that, in Cu/TiO₂ interface, the galvanic couple existes and Cu acts as the anode while it acts as the cathode. It can be concluded that the potential difference between Cu and TiO₂, corrosion process of Cu is accelerating, especially the corrosion rate of the area adjacent to TiO₂ particles. It can be predicted that corrosion of TiO₂ particles is extremely slight, and its main corrosion type could be pitting. Usually, cuprous oxide is formed when copper and oxygen react in presence of chloride ions. But increase in ceramic particles increases the rate of corrosion as the oxidation reaction speeds up due to the presence of more oxide particles in the layer and formation of thick unstable copper peroxide layer. Since the time for passivating layer (Cuprous oxide) to form is greater than the time for oxide layer (Copper peroxide) to form, degradation was more on the top layer of the composite which was also observed in some previous works^{13,24,27}. This could also be seen in the decreasing polarization resistance value. It may be inferred that the increasing in ceramic particles content the copper metal matrix composite was more susceptible to corrosion and becomes unsuitable for use in corrosive environments¹³.

Conclusions

Copper metal matrix nanocomposite has desirable properties for various applications such as heating and cooling systems, pipelines and drinking vessels. Cu-based nanocomposites with different wt.% of TiO₂ were fabricated and their properties were evaluated. The Cu density was decreased due to add TiO₂ nanoparticles. In addition, the experimental densities of fabricated specimens were lower than the theoretical densities of all test specimens. This is because the fabricated nanocomposites may contain some porosity. The hardness of pure Cu was 53 HV, and increased to 91 HV, in Cu-based nanocomposite with 12 wt.% TiO₂ with improving ratio 71.7%.

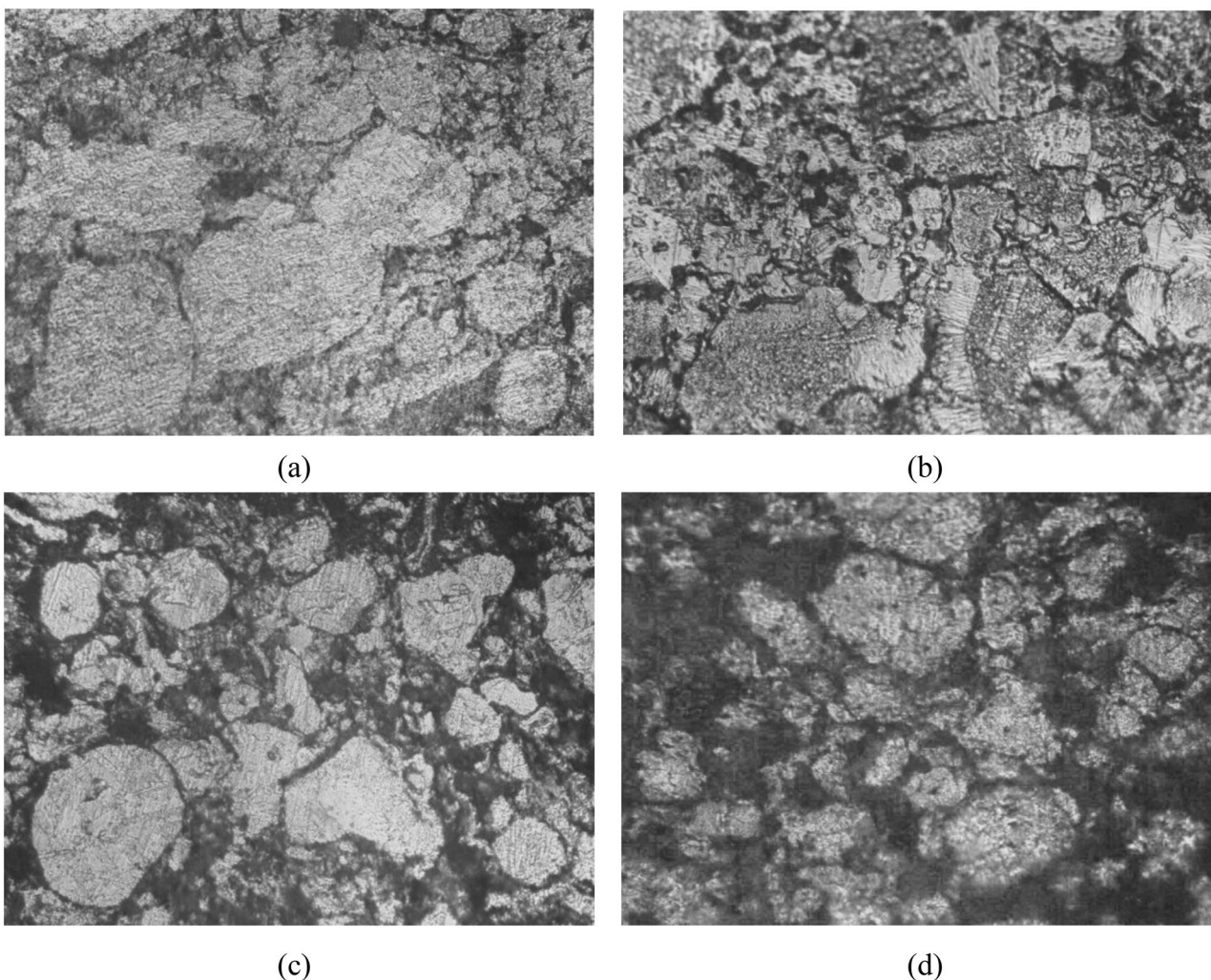


Figure 14. Corroded surfaces of C/TiO₂ nanocomposites, in 3.5% NaCl solution, X200; (a) 0% TiO₂, (b) 4% TiO₂, (c) 8% TiO₂, (d) 12% TiO₂.

The electrochemical measurements of pure Cu and Cu reinforced with 0, 4, 8 and 12wt% TiO₂ nano particles was studied in 3.5% NaCl, 0.5 M NaOH and 0.5 M H₂SO₄ solutions by Potentiodynamic polarization curves and electrochemical impedance spectroscopy (EIS). The corrosion current density of pure Cu increases with the increasing of TiO₂ nanoparticles percentage in all tested solutions. In addition, the corrosion current density of all test specimens in 0.5 M H₂SO₄ solution was higher than the corrosion current density of test specimens in both 0.5 M NaOH and 3.5% NaCl solutions. This is because the acidic solution is more severe than both the alkaline and salty solutions. The results of the measured impedance for the pure Cu and Cu matrix composites in 3.5% NaCl, 0.5 M NaOH, and 0.5 H₂SO₄ solutions confirm the results obtained from the potentiodynamic polarization curve. Furthermore, the specimens' resistance values R_p and R_u in the 3.5% NaCl solution are larger than those in the 0.5 M NaOH and 0.5 H₂SO₄ solutions. It can be concluded that Cu matrix composites reinforced with TiO₂ particles may be promising materials due to their excellent mechanical and physical properties. However the corrosion behavior need more studies.

Received: 28 January 2022; Accepted: 8 April 2022
Published online: 23 April 2022

References

1. Koontz, J. L., Liggans, G. L. & Redan, B. W. Temperature and pH affect copper release kinetics from copper metal foil and commercial copperware to food simulants. *Food Addit. Contamin.: Part A* 37(3), 465–477 (2020).
2. Simonson, R. 2016 Jul 18. At age 75, the moscow mule gets its kick back. New York Times. Sect. Food. <https://www.nytimes.com/2016/07/20/dining/moscow-ule.html>
3. Sovich, N. 2016 Jun 7. The cast iron and copper pot comeback. Wall St Journal. Sect. Life & Style. <https://www.wsj.com/articles/the-cast-iron-and-copper-pot-comeback-1465328926>
4. Al-Abdallah, M. M., Maayta, A. K., Al-Qudahand, M. A. & Al-Rawashdeh, N. A. F. Corrosion behavior of copper in chloride media. *Open Corrosion J.* 2, 71–76 (2009).

5. Elmahdy, M., Abouelmagd, G. & Mazen, A. A. E. Microstructure and properties of Cu–ZrO₂ nanocomposites synthesized by in situ processing. *Mater. Res.* **21**(1), e20170387 (2018).
6. El-Aiat, M.M., Abdel-Karim, R., Kandel, A.A. & Saber, D. Erosive–corrosive behavior of A356 alloy reinforced by alumina particles. In MEATIP5, Conference, March 29–31, Cairo, Egypt, pp. 137–151 (2011).
7. Saber, D. Improvement of tribological properties of A356–Al₂O₃ cast composites by heat- treatment. *J. Al-Azhar Univ. Eng. Sect.* **13**, 998 (2018).
8. Hossain, S., Rahman, M. M. & Chawla, D. Fabrication, microstructural and mechanical behavior of Al- Al₂O₃-SiC hybrid metal matrix composites. *Mater Today Proc* **21**, 1458–1461 (2020).
9. Megahed, M., Saber, D. & Agwa, M. A. Modeling of wear behavior of Al-Si/Al₂O₃ metal matrix composites. *Phys. Met. Metall.* **120**(10), 981–988 (2019).
10. Moghanian, A. *et al.* Production and properties of Cu/TiO₂ nano-composites. *J. Alloys Compd.* **698**, 518–524 (2017).
11. Ning, D., Zhang, A. & Wu, H. Cu–TiO₂ composites with high incorporated and uniform distributed TiO₂ particles prepared by jet electrodeposition. *Surf. Eng.*, 1–7 (2019).
12. Toptan, F., Alves, A. C., Kerti, I., Ariza, E. & Rocha, L. A. “Corrosion and tribo corrosion behavior of Al–Si–Cu–Mg alloy and its composites reinforced with B4C particles in 0.05 M NaCl solution. *Wear* **306**, 27 (2013).
13. Rajesh kumar, L. & Amirthagadeswaran, K. S. Corrosion and wear behaviour of nano Al₂O₃ reinforced copper metal matrix composites synthesized by high energy ball milling. *Particulate Sci. Technol.* **38**(2), 228–235 (2020).
14. Zawrah, M. F., Zayed, H. A., Essawy, R. A., Nassar, A. H. & Taha, M. A. Preparation by mechanical alloying, characterization and sintering of Cu–20 wt.% Al₂O₃ nanocomposites. *Mater. Des.* **46**, 485 (2013).
15. Norouzfard, V., Naeinzadeh, H., Talebi, A. & Ebrahimi, Z. Microstructure, mechanical and electrical properties of copper matrix composites reinforced with steel nanoparticles. *Mech. Adv. Compos. Struct.* **8**, 335–345 (2021).
16. Hamid, F. S. *et al.* Analysis of microstructure and mechanical properties of bi-modal nanoparticle-reinforced Cu-matrix. *Curr. Comput.-Aided Drug Des.* **11**, 1081. <https://doi.org/10.3390/cryst11091081> (2021).
17. Zhang, Z. G., Sheng, Y. Y., Xu, X. W. & Li, W. Microstructural features and mechanical properties of in situ formed ZrB₂/Cu composites. *Adv. Eng. Mater.* **17**, 1338–1343 (2015).
18. Wang, C. C., Lin, H. J., Zhang, Z. G. & Li, W. Fabrication, interfacial characteristics and strengthening mechanisms of ZrB₂ micro-particles reinforced Cu composites prepared by hot-pressed sintering. *J. Alloy Compd.* **748**, 546–1522 (2018).
19. Ezhil Singh, S. C. & Selvakumar, N. Effect of milled B 4 C Nano particles on tribological analysis, microstructure and mechanical properties of Cu 4Cr matrix produced by hot extrusion. *Arch. Civil Mech. Eng.* **17**, 446–456 (2017).
20. Fathy, A., Shehata, E., Abdelhameed, M. & Elmahdy, M. Compressive and wear resistance of nanometric alumina reinforced copper matrix composites. *Mater. Des.* **36**, 100–107 (2012).
21. Efe, G. C., Ipek, M., Zeytin, S. & Bindal, C. An investigation of the effect of SiC particle size on Cu-SiC composites. *Compos. B Eng.* **43**(4), 1813–1822 (2012).
22. Hidalgo-Manrique, P. *et al.* Copper/graphene composites: a review. *J. Mater. Sci.* **54**, 12236–12289 (2019).
23. Sorkhe, Y. A., Aghajani, H. & Taghizadeh Tabrizi, A. Mechanical alloying and sintering of nanostructured TiO₂ reinforcedcopper composite and its characterization. *Mater. Design* **58**, 168–174 (2014).
24. Golnaz, N. A., Arvin, T. T. & Aghajani, H. Investigation on corrosion behavior of Cu–TiO₂ nanocomposite synthesized by the use of SHS method. *J. Mater. Res. Technol.* **8**(2), 2216–2222 (2019).
25. Saber, D., Fathy, A. & Abdel-Aziz, Kh. A study of corrosion behavior of copper-alumina nanocomposites in different corrosive media. *Int. J. Mech. Eng. (IJME)* **5**, 1–10 (2016).
26. Dobrzanski, L. A., Włodarczyk, A. & Adamiak, M. Structure, properties and corrosion resistance of PM composite materials based on EN AW-2124 aluminum alloy reinforced with the Al₂O₃ ceramic particles. *J. Mater. Process. Technol.* **27**, 162–163 (2005).
27. Saber, D., Abd El-Aziza, K., Abdel-Karim, R. & Kandel, A. A. Corrosive wear of alumina particles reinforced Al–Si alloy composites. *Phys. Metals Metallography* **121**, 197–203 (2020).
28. Mirsaeed-Ghazi, S. M., Allahkaram, S. R. & Molaei, A. Tribological behavior and corrosion properties of graphite incorporated Cu/Sic nanocomposite coatings prepared by pulse current electrodeposition. *Inorg. Chem. Ind. J.* **13**(1), 123 (2018).
29. Baghani, M., Aliofkhaezai, M. & Askari, M. Cu–Zn–Al₂O₃ nanocomposites: study of microstructure, corrosion, and wear properties. *Int. J. Min. Metallurgy Mater.* **24**(4), 462 (2017).
30. Hosseini, J. & Bodaghi, A. Corrosion behaviour of electroless Ni–P–TiO₂ nanocomposite coatings using taguchi. *Surf. Eng.* **29**(3), 183–189 (2013).
31. Ajeel, S. A., Yaseen, R. S. & KEqal, A. Improvement the corrosion resistance of aluminum bronze alloy (Cu-7.7 wt.% Al) reinforced by Al₂O₃ and TiO₂ nanoparticles. *IOP Conf. Series: Materials Science and Engineering* **518**, 032046 (2019)
32. Raghav, G. R., Selvakumar, N., Jeyasubramanian, K. & Thansekhar, M. R. Corrosion analysis of copper -TiO₂ nanocomposite coatings on steel using sputtering. *Int. J. Innov. Res. Sci. Eng. Technol.* **3**, 3 (2014).
33. Saif, S., Irhayyim1, Hashim, Hammood, Sh., Hassan & Abdulhadi, A. Effect of nano-TiO₂ particles on mechanical performance of Al–CNT matrix composite. *AIMS Materials Science*, **3M**.
34. Almomani, A., Shatnawi, A.M. & Alrashdan, M.K. Effect of sintering time on the density, porosity content and microstructure of copper – 1 wt. % silicon carbide composites. *Adv. Mater. Res.* **1064**, 32.6(6):1124–1134 (2019).
35. Ali, M. & Falih, S. Synthesis and characterization of aluminum composites materials reinforced with TiC nano- particles. *Jordan J. Mech. Indu. Eng.* **8**(5), 257–264 (2014).
36. Kamrani, S., Riede, R., Reihani, S. & Kleebe, A. Effect of reinforcement volume fraction on the mechanical properties of Al-SiC nanocomposites produced by mechanical alloying and consolidation. *J. Compos. Mater.* **44**, 1–14 (2009).
37. Koti, V., George, R., Shakiba, A. & ShivanandaMurthy, K. V. Mechanical properties of copper nanocomposites reinforced with uncoated and nickel coated carbon nanotubes. *FME Trans.* **46**, 623–630 (2018).
38. Saber, D., Ibrahim, Taha, B.M. & Abd El-Aziz, Kh. Prediction of the corrosion rate of Al–Si alloys using optimal regression methods. *Intell. Autom. Soft Comput.* (2021)
39. Abd El-Aziz, K., Saber, D. & Sallam, H. E. M. Wear and corrosion behavior of Al–Si matrix composite reinforced with alumina. *Springerlink. J. Bio- Tribo-Corrosion* **1**, 5 (2015).
40. Kear, G., Barker, B. D. & Walsh, F. C. Electrochemical corrosion of unalloyed copper in 503 chloride media—A critical review. *Corros. Sci.* **46**, 109–135 (2004).
41. Khaleel, K. F. Studies of the corrosion inhibition of copper in sodium chloride solutions using chemical and electrochemical measurements. *Mater. Chem. Phys.* **125**, 427–433 (2011).
42. Zafarany, I. & Boller, H. Electrochemical behavior of copper electrode in sodium hydroxide solutions. *Current World Environ.* **4**, 277–284 (2009).
43. M. Pourbaix, Atlas of Electrochemical Equilibria in Aqueous Solutions, 2nd ed., National Association of Corrosion Engineers, Houston, Texas, USA, 77084, 1974.
44. Xometl, O. O. *et al.* Thiadiazoles as corrosion inhibitors for carbon steel in H₂SO₄ solutions. *Int. J. Electrochem. Sci.* **8**, 735–752 (2013).
45. Nagendra Prasad, Y., Vinod Kumar, V. & Ramanathan, S. Electrochemical impedance spectroscopic studies of copper dissolution in arginine–hydrogen peroxide solutions. *J. Solid State Electrochem.* **13**, 1351–1359 (2009).

46. Abd ElAziz, Kh., Ahmed, E.M., Alghtani, A.H., Felemban, B.F., Ali, H.T. & M Megahed, D Saber, "Development of Al-Mg-Si alloy performance by addition of grain refiner Al-5Ti-1B alloy" *Science Progress*, 104(2) (2021).
47. Wheat, H.G. "Corrosion Behavior Of Metal Matrix Composites", final Report For The Period July 1, 1989 Through September 1992.
48. Arsenault, R.J. In metal matrix composites: mechanisms and properties. In R.K. Everett and R.J. Arsenault, Ed., Academic Press (1991), 79.
49. Loto, R. T. & Adeleke, A. Corrosion of aluminum alloy metal matrix composites in neutral chloride solutions. *J. Fail. Anal. Prev.* **16**, 874–885 (2016).
50. Xie, Z., Guo, H., Zhang, X. & Huang, S. Corrosion behavior of pressure infiltration Diamond/Cu composites in neutral salt spray. *Materials* **13**, 1847 (2020).
51. Monje, I. E., Louis, E. & Molina, J. M. Role of Al₄C₃ on the stability of the thermal conductivity of Al/diamond composites subjected to constant or oscillating temperature in a humid environment. *J. Mater. Sci.* **51**, 8027–8036 (2016).
52. Jin, B. *et al.* Enhanced corrosion resistance in metal matrix composites assembled from graphene encapsulated copper nanoflakes. *Carbon* **142**, 482–490 (2019).

Acknowledgements

The authors would like to thank Taif University for its financial support. This research was fully funded by the Deanship of Scientific Research, Taif University, KSA. [Research group number 1-441-92].

Author contributions

Kh.A., M.M., and D.S. wrote the main manuscript text, E.A., B.F. and A.A. prepared literature review, Kh.A. and H.A. prepared experimental work, All authors reviewed the manuscript.

Competing interests

The authors declare no competing interests.

Additional information

Correspondence and requests for materials should be addressed to D.S.

Reprints and permissions information is available at www.nature.com/reprints.

Publisher's note Springer Nature remains neutral with regard to jurisdictional claims in published maps and institutional affiliations.



Open Access This article is licensed under a Creative Commons Attribution 4.0 International License, which permits use, sharing, adaptation, distribution and reproduction in any medium or format, as long as you give appropriate credit to the original author(s) and the source, provide a link to the Creative Commons licence, and indicate if changes were made. The images or other third party material in this article are included in the article's Creative Commons licence, unless indicated otherwise in a credit line to the material. If material is not included in the article's Creative Commons licence and your intended use is not permitted by statutory regulation or exceeds the permitted use, you will need to obtain permission directly from the copyright holder. To view a copy of this licence, visit <http://creativecommons.org/licenses/by/4.0/>.

© The Author(s) 2022